Magnetic and Mössbauer spectral evidence for the suppression of the magnetic spin reorientation in Tm_2Fe_{17} by deuterium

Fernande Grandjean*
Institut de Physique, B5, Université de Liège, B-4000 Sart-Tilman, Belgium

Olivier Isnard†
Laboratoire de Cristallographie du CNRS, associé à l'Université J. Fourier et à l'INPG, CNRS, F-38042 Grenoble, France

Gary J. Long‡
Department of Chemistry, University of Missouri-Rolla, Rolla, Missouri 65409-0010

(Received 9 August 2001; revised manuscript received 29 October 2001; published 22 January 2002)

The structural and magnetic properties of Tm_2Fe_{17} and $Tm_2Fe_{17}D_{3.2}$ are investigated by means of x-ray-diffraction, thermal, and ac magnetic susceptibility measurements, and iron-57 Mössbauer spectroscopy. Both compounds crystallize in a hexagonal $P6_3/mmc$ space group with a Th_2Ni_{17}-like structure. Deuterium insertion into Tm_2Fe_{17} induces large increases in the unit-cell volume, the saturation magnetization, and the ordering temperature. The unit-cell expansion is anisotropic, with a larger increase in the *a* lattice parameter than the *c* lattice parameter. A spin reorientation is observed at 90 K in Tm_2Fe_{17} in the temperature dependence of both the ac susceptibility and the Mössbauer spectra. Above and below 90 K, the iron magnetic moments are aligned within the basal plane and along the *c*-axis, respectively. An analysis of the Mössbauer spectra from 4.2 to 320 K yields the orientation of the iron magnetic moments and hyperfine fields, relative to the axes of the electric-field gradient tensor at the iron sites. As revealed by both the ac susceptibility measurements and the Mössbauer spectra, deuterium insertion into Tm_2Fe_{17} suppresses this spin reorientation, and in $Tm_2Fe_{17}D_{3.2}$ the iron magnetic moments are oriented within the basal plane of the unit cell from 4.2 to 295 K. The spin reorientation in Tm_2Fe_{17} results from a competition between the thulium and iron magnetic anisotropies. Below 90 K the thulium anisotropy dominates and favors an axial alignment of the spins. In contrast to carbon and nitrogen, deuterium insertion into Tm_2Fe_{17} decreases the influence of the thulium anisotropy, and in $Tm_2Fe_{17}D_{3.2}$ the iron anisotropy dominates and favors a basal alignment of the magnetic moments.

DOI: 10.1103/PhysRevB.65.064429 PACS number(s): 75.50.Bb, 75.50.Gg, 76.80.+y

I. INTRODUCTION

In the series of R_2Fe_{17} compounds and their hydrides, Tm_2Fe_{17} plays a special role because of its spin reorientation[1–3] below 100 K. Indeed, neutron-diffraction measurements[4] have shown that below the critical temperature, the iron magnetic moments in Tm_2Fe_{17} are aligned parallel to the *c* axis of the hexagonal unit cell, whereas, above the critical temperature, they are aligned within the basal plane of the hexagonal unit cell. This spin reorientation was also confirmed[5] in an early Mössbauer spectral study.

The insertion of hydrogen or deuterium into the R_2Fe_{17} compounds is known[6] to dramatically influence their magnetic properties. Further, the insertion of carbon or nitrogen into Tm_2Fe_{17} substantially increases[3,7,8] its spin reorientation temperature. Hence it is of importance to investigate the effect of hydrogen or deuterium on the magnetic properties of Tm_2Fe_{17}.

We have carried out a systematic magnetic and Mössbauer spectral study of the R_2Fe_{17} compounds and their hydrides, for $R=$Ce,[9] Pr,[10,11] Nd,[12] Sm,[13] Gd,[13] Dy,[14] and Er.[15] For light rare-earth elements from Ce to Gd, the R_2Fe_{17} compounds and their hydrides crystallize in the rhombohedral $R\text{-}3m$ space group with a Th_2Zn_{17}-like structure, whereas for heavy rare-earth elements, from Dy to Tm, they crystallize in the hexagonal $P6_3/mmc$ space group with a Th_2Ni_{17}-like structure. Although the rhombohedral compounds are very close to stoichiometric and show completely ordered crystal structures, the hexagonal compounds are usually iron rich and often have disordered crystal structures, a disorder which can be observed in the Mössbauer spectra, as shown in our previous studies.[14,15] Various magnetic and dynamic phenomena induced by the insertion of hydrogen, such as spin reorientations, Curie temperature increases, and hydrogen motions, were also observed in the Mössbauer spectra[10–15] of these compounds and their hydrides.

In the course of our Mössbauer spectral study of the R_2Fe_{17} compounds and their hydrides, we have analyzed the spectra with a self-consistent model, a model which is based on the orientation of the iron magnetic moments, the correlation between the iron isomer shifts and the Wigner-Seitz cell volumes, and the correlation between the hyperfine fields and the number of iron near neighbors. Unfortunately, because none of the R_2Fe_{17} compounds studied so far exhibit an axial orientation of the iron magnetic moments, no detailed analysis or discussion of the quadrupole interactions and the orientation of the hyperfine field within the electric-field gradient tensor axes was possible. However, in Tm_2Fe_{17} the iron magnetic moments are oriented parallel to the *c* axis below 90 K and its Curie temperature is low at 280 K; as a consequence, a detailed analysis is possible and is reported herein. Unfortunately, the rather limited resolution of an ear-

TABLE I. Lattice parameters, unit-cell volume, and magnetic transition temperatures.

Compound	a (Å)	c (Å)	V (Å^3)	T_{sr} (K)	T_C (K)
Tm_2Fe_{17}	8.420(2)	8.272(2)	507.9	90(5)	280(8)
$Tm_2Fe_{17}D_{3.2}$	8.537(2)	8.311(2)	524.5	-	465(5)
% increase	1.39	0.47	3.27		66

lier Mössbauer spectral study[2,5] of Tm_2Fe_{17} did not permit a complete discussion of the hyperfine parameters.

II. EXPERIMENT

Polycrystalline Tm_2Fe_{17} was prepared by high-frequency induction melting of elements of 99.9% or better purity. The melting was carried out in a cold copper crucible under an argon atmosphere. Because of the high vapor pressure of thulium, a small excess of thulium was used in order to improve the stoichiometry of the product and to minimize its α-Fe content. Sample homogeneity was optimized by wrapping small pieces of the induction melted ingot in tantalum foil, sealing them in evacuated silica tubes, and annealing them at 1270 K for at least two weeks. The resulting ingot was slightly stoichiometrically rich in iron, leading to an actual ingot composition of $Tm_2Fe_{17.6}$, a composition which corresponds to Tm_2Fe_{17} and 2.1 wt % of excess iron, or to an iron-rich $Tm_{2-z}Fe_{17+2z}$ phase and less excess iron. The homogeneity range of the R_2Fe_{17} compounds, where R is a heavy rare earth, is known[16] to broaden with increasing rare-earth atomic number. For the sake of simplicity, this compound will be referred to as Tm_2Fe_{17} rather than by its actual stoichiometry.

The insertion of deuterium into Tm_2Fe_{17} to form $Tm_2Fe_{17}D_{3.2}$ has been carried out at 370 K in a stainless-steel autoclave at a pressure of ~5 MPa. The deuterium content was controlled by measuring the deuterium vapor pressure change above the sample, and the final deuterium content was obtained from a gravimetric analysis. The use of deuterium as opposed to hydrogen makes this gravimetric analysis more accurate. The deuterium content accuracy is $\sim\pm0.1$ deuterium atom per formula unit, an accuracy which was confirmed[16,17] by earlier neutron-diffraction studies of related R_2Fe_{17} deuterides and hydrides.

The purity of the samples was confirmed by powder x-ray diffraction. The samples were found to be single phase with traces of α-iron. High accuracy lattice parameters were obtained with a Guinier-type focusing camera and iron $K\alpha_1$ radiation. Powdered silicon was added as an internal standard. The lattice parameters and unit-cell volumes are given in Table I. The expansion of the unit-cell volume upon the insertion of deuterium is ~3.3%, an expansion which is smaller than is observed[9,10,16] for the R_2Fe_{17} compounds with light rare earths which can accommodate up to five hydrogen or deuterium atoms per formula unit. This expansion occurs anisotropically with a much larger increase in the a than the c lattice parameter.

The 465 K magnetic ordering temperature T_C of $Tm_2Fe_{17}D_{3.2}$ was obtained on a Faraday torque balance with 5 K per minute heating or cooling. A sample of ~50 mg was sealed under vacuum in a small silica tube in order to prevent oxidation of the sample during heating. The magnetic ordering temperature of Tm_2Fe_{17} is 280 K, as determined by low temperature ac susceptibility measurements. There is a substantial increase of 185 K in the ordering temperature upon deuterium insertion into Tm_2Fe_{17}, an increase which results from the negative pressure effect of the interstitial element on the lattice. The relative increase of 20% per inserted deuterium atom is larger than that usually observed[18] for the R_2Fe_{17} compounds, and is probably a consequence of the smaller unit-cell volume of Tm_2Fe_{17}. Hence, the insertion of deuterium into Tm_2Fe_{17} is more effective in increasing the iron-iron exchange interactions than it is in the other R_2Fe_{17} compounds.

The 4.2–295 K ac magnetic susceptibilities were obtained on a computer controlled mutual inductance susceptometer[19] at an exciting field of 1 Oe and a frequency of 120 Hz. A lock-in amplifier was used to measure the complex susceptibility, $\chi_{ac}=\chi'-j\chi''$, where χ' is the initial susceptibility, a quantity which is related to the variation in the sample magnetization, and χ'' is nonzero if the magnetic energy is absorbed by the sample. The saturation magnetization has been obtained[20] at 5 and 295 K by the extraction method in continuous fields ranging up to 7 T.

Mössbauer spectral absorbers of ~36 mg/cm^2 were prepared from powdered samples which were sieved to a 0.045-mm or smaller diameter particle size. The Mössbauer spectra were obtained between 4.2 and 320 K on a constant-acceleration spectrometer which utilized a rhodium matrix cobalt-57 source, and was calibrated at room temperature with α-iron foil. The studies were carried out in a Janis Supervaritemp cryostat in which the samples were never exposed to a vacuum. The spectra were fit as discussed below, and the estimated relative errors were at most ±1 kOe for the hyperfine fields, ±0.002 mm/s for the isomer shifts, ±0.01 mm/s for the quadrupole interactions, $\pm5°$ for the θ angles, ±0.005 mm/s for the linewidths, and $\pm0.5\%$ for the relative spectral component areas. The absolute errors are larger by a factor of approximately 2.

III. MAGNETIC RESULTS

The magnetization curves for Tm_2Fe_{17} and $Tm_2Fe_{17}D_{3.2}$ are shown in Fig. 1. The saturation magnetization at 5 K is $20.2\mu_B$ and $24.4\mu_B$ per formula unit for Tm_2Fe_{17} and $Tm_2Fe_{17}D_{3.2}$, respectively. Whereas the magnetization of $Tm_2Fe_{17}D_{3.2}$ is saturated in an applied field of 20 kOe, that of Tm_2Fe_{17} is not fully saturated in an applied field of 70 kOe. This different behavior probably originates in the tendency of the dumbbell iron sites to favor antiferromagnetic interactions between themselves.[4,21–23] It should be noted that the magnetization of $Tm_2Fe_{17}D_{3.2}$ at 300 K is $27.3\mu_B$ per formula unit, and higher than that observed at 5 K because of the decrease in the antiferromagnetic contribution of the thulium sublattice to the total magnetization at 300 K. This antiferromagnetic contribution is emphasized in the inset of Fig. 1 showing the temperature dependence of the magnetization measured at 30 kOe in Tm_2Fe_{17} and

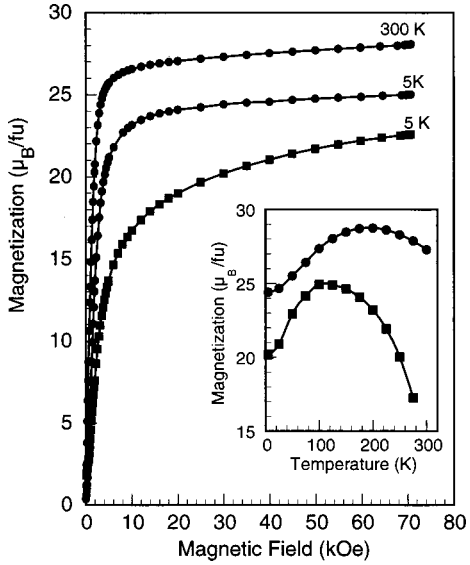

FIG. 1. The magnetization curves for Tm_2Fe_{17} obtained at 5 K (squares), and for $Tm_2Fe_{17}D_{3.2}$ (circles), obtained at 5 and 300 K. Inset: the temperature dependence of the magnetization measured at 30 kOe for Tm_2Fe_{17} (squares), and $Tm_2Fe_{17}D_{3.2}$ (circles).

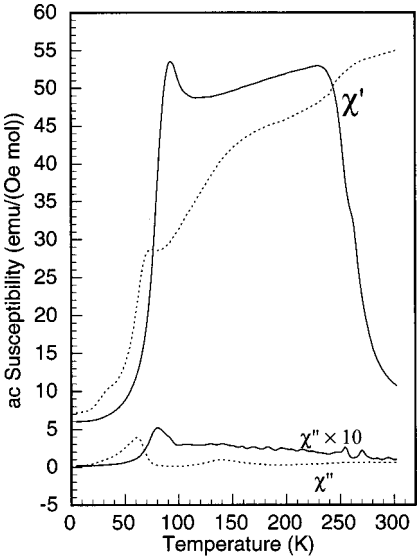

FIG. 2. The temperature dependence of the real, χ', and imaginary, χ'', portions of the ac magnetic susceptibility of Tm_2Fe_{17} (solid lines), and $Tm_2Fe_{17}D_{3.2}$ (dotted lines).

$Tm_2Fe_{17}D_{3.2}$. If the magnetic moment of thulium is assumed to be equal to the free ion value in both Tm_2Fe_{17} and $Tm_2Fe_{17}D_{3.2}$, then the increase in saturation magnetization of $4.2\mu_B$ per formula unit in going from Tm_2Fe_{17} to $Tm_2Fe_{17}D_{3.2}$ can be attributed to an increase in the iron sublattice magnetization. This rather large increase more likely results from an improved ferromagnetic alignment of the iron magnetic moments rather than from an increase in iron magnetic moments, as indicated by the Mössbauer hyperfine fields; see below. In contrast, in the $Y_2Fe_{17}H_x$ and $Lu_2Fe_{17}D_x$ compounds, in which the yttrium and lutetium are nonmagnetic, only a small change of the iron sublattice magnetization with x has been observed.[18]

In a search for a spin reorientation, ac susceptibility measurements between 4.2 and 300 K have been performed on Tm_2Fe_{17} and $Tm_2Fe_{17}D_{3.2}$; see Fig. 2. Indeed, this technique is known[24] to be very sensitive to changes in the magnetization direction in rare-earth and transition-metal intermetallic compounds. The dramatic drop at ~274 K in the ac susceptibility of Tm_2Fe_{17} is associated with a ferromagnetic to paramagnetic transition. The ordering temperature of $Tm_2Fe_{17}D_{3.2}$ of 465 K is beyond the investigated temperature range of Fig. 2.

As expected for a spin reorientation, both the real and imaginary parts of the ac susceptibility of Tm_2Fe_{17} exhibit both a peak and a discontinuity at ~90 K. A similar dependence of the ac susceptibility was observed[25] for the $Tm_2Fe_{17}C_x$ series of compounds. The real part of the ac susceptibility of Tm_2Fe_{17} is characterized by two regimes. First, at low temperatures small values of the ac susceptibility are observed when the easy magnetization direction is aligned along the c axis of the structure. Second, above the ~90 K spin reorientation temperature, much higher susceptibilities are observed when the easy magnetization axis is within the basal plane of the structure. In contrast, $Tm_2Fe_{17}D_{3.2}$ exhibits a continuous decrease in the ac susceptibility on cooling (see Fig. 2), and only weak anomalies, reminiscent of those observed[14,15] in Dy_2Fe_{17} and Er_2Fe_{17}, are observed in the real part of the ac susceptibility. It is worth noting that the shoulder present at 70 K in the ac susceptibility of $Tm_2Fe_{17}D_{3.2}$ is similar to that observed[15] in Er_2Fe_{17} and $Er_2Fe_{17}H_3$, both of which show a basal orientation of the magnetization between 4.2 and 300 K.

IV. MÖSSBAUER SPECTRAL RESULTS

Tm_2Fe_{17}. The Mössbauer spectra of Tm_2Fe_{17} obtained at 295 and 320 K are paramagnetic, and the 320 K spectrum is shown in Fig. 3. These spectra are very similar to the paramagnetic spectra[9,15] of Ce_2Fe_{17} and Er_2Fe_{17} and have been analyzed with five doublets assigned to the $4e$, $4f$, $6g$, $12j$, and $12k$ sites; and one additional doublet representing the inner lines of the α-iron impurity. The isomer shifts, δ, quadrupole splittings ΔE_Q, and relative areas of these doublets are given in Table II. A single linewidth of 0.29 mm/s has been adjusted, and the relative areas of the $6g$, $12j$, and $12k$

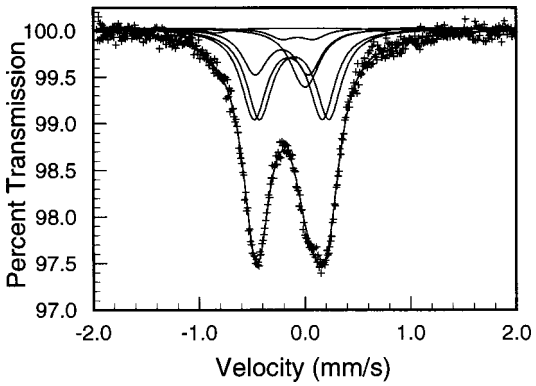

FIG. 3. The Mössbauer spectrum of Tm_2Fe_{17} obtained at 320 K.

TABLE II. Mössbauer spectral hyperfine parameters for Tm_2Fe_{17}.

	T, K	$4f$	$4e$	$6g_4$	$6g_2$	$12j_8$	$12j_4$	$12k_8$	$12k_4$	Wt. Ave.
H, kOe	4.2	417.7	382.0	329.0	329.0	293.5	293.5	331.7	331.7	329.7
	45	410.0	377.0	322.0	322.0	288.0	288.0	326.0	326.0	323.7
	60	400.2	371.0	316.0	316.0	283.0	283.0	320.0	320.0	317.6
	70	394.7	367.0	311.0	311.0	278.5	278.5	315.2	315.2	312.8
	85	388.9	362.3	306.9	306.9	275.5	275.5	312.4	312.4	309.3
	90	387.2	360.0	304.0	304.0	273.9	273.9	309.5	309.5	307.0
	95	356.2	372.0	276.3	295.3	275.4	310.3	296.2	253.9	295.6
	100	343.0	362.0	271.1	290.0	272.3	307.9	291.7	248.6	290.3
	120	333.2	351.0	261.2	275.9	261.3	300.9	281.0	235.6	279.6
	155	312.0	334.0	246.0	259.3	245.1	285.9	265.4	220.7	263.4
	225	253.1	270.0	196.3	206.1	192.3	233.0	212.3	210.2	210.2
δ,[a] mm/s	4.2	0.220	0.175	−0.082	−0.082	0.008	0.008	0.062	0.062	0.041
	45	0.218	0.170	−0.077	−0.077	0.005	0.005	0.060	0.060	0.040
	60	0.216	0.165	−0.078	−0.078	−0.002	−0.002	0.057	0.057	0.036
	70	0.215	0.160	−0.080	−0.080	−0.004	−0.004	0.056	0.056	0.034
	85	0.205	0.155	−0.078	−0.078	−0.015	−0.015	0.048	0.048	0.027
	90	0.195	0.150	−0.078	−0.078	−0.020	−0.020	0.040	0.040	0.021
	95	0.180	0.150	−0.090	−0.090	−0.030	−0.030	0.000	0.000	0.000
	100	0.175	0.150	−0.085	−0.085	−0.035	−0.035	−0.005	−0.005	−0.003
	120	0.165	0.140	−0.090	−0.090	−0.045	−0.045	−0.008	−0.008	−0.010
	155	0.155	0.110	−0.100	−0.100	−0.060	−0.060	−0.015	−0.015	−0.021
	225	0.100	0.060	−0.140	−0.140	−0.100	−0.100	−0.055	−0.055	−0.063
	295	0.020	−0.050	−0.205	−0.205	−0.145	−0.145	−0.075	−0.075	−0.109
	320	0.005	−0.065	−0.215	−0.215	−0.155	−0.155	−0.100	−0.100	−0.125
$e^2Qq/2$, mm/s	4.2	−0.09	−0.30	−0.52	−0.52	0.56	0.56	−0.56	−0.56	-
	45–95	−0.14	−0.30	−0.52	−0.52	0.56	0.56	−0.56	−0.56	-
	100–225	−0.12	−0.30	−0.52	−0.52	0.58	0.58	−0.56	−0.56	-
ΔE_Q, mm/s	295	−0.08	−0.30	−0.52	-	0.66	-	−0.65	-	-
	320	−0.08	−0.30	−0.51	-	0.66	-	−0.65	-	-
η	4.2–90	0	0	0	0	1	1	1	1	-
	95–225	0	0	0	0	0.7	0.7	0.85	0.85	-
θ, deg	4.2–90	0	0	60	60	66	66	0	0	-
	95–100	90	90	42	0	42	90	80	90	-
	120	90	90	48	0	34	90	84	90	-
	155–225	90	90	48	0	36	90	86	90	-
Area, %	4.2	14.2	4.2	10.9	5.4	21.7	10.9	21.7	10.9	-
	45	13.7	4.1	10.9	5.4	22.0	11.0	22.0	11.0	-
	60	13.5	4.3	10.9	5.4	22.0	10.9	22.0	10.9	-
	70	12.9	4.5	11.0	5.6	22.0	11.0	22.0	11.0	-
	85	11.2	5.7	11.0	5.6	22.0	11.1	22.0	11.1	-
	90	10.0	5.3	11.3	5.6	22.7	11.3	22.7	11.3	-
	95	8.5	4.7	11.6	5.8	23.2	11.6	23.2	11.6	-
	100	11.8	3.9	11.3	5.2	22.5	11.3	22.5	11.3	-
	120	11.0	4.2	11.3	5.7	22.6	11.3	22.6	11.3	-
	155	11.9	3.4	11.3	5.6	22.6	11.3	22.6	11.3	-
	225	9.4	5.8	11.3	5.8	22.5	11.3	22.5	11.3	-
	295	10.7	6.3	16.2	-	32.4	-	32.4	-	-
	320	12.2	3.8	16.8	-	33.6	-	33.6	-	-

[a]The isomer shifts are given relative to room temperature α-iron foil.

doublets have been constrained in the ratio 6:12:12. The signs of the quadrupole interactions are determined from the analysis of the magnetic spectra, see below.

The Mössbauer spectra of Tm_2Fe_{17}, obtained at 4.2, 45, 70, 100, and 225 K, are shown in Fig. 4. The obvious changes in the shape of the spectra obtained between 70 and 100 K are due to the spin reorientation and the associated change in the number of magnetically inequivalent iron sites

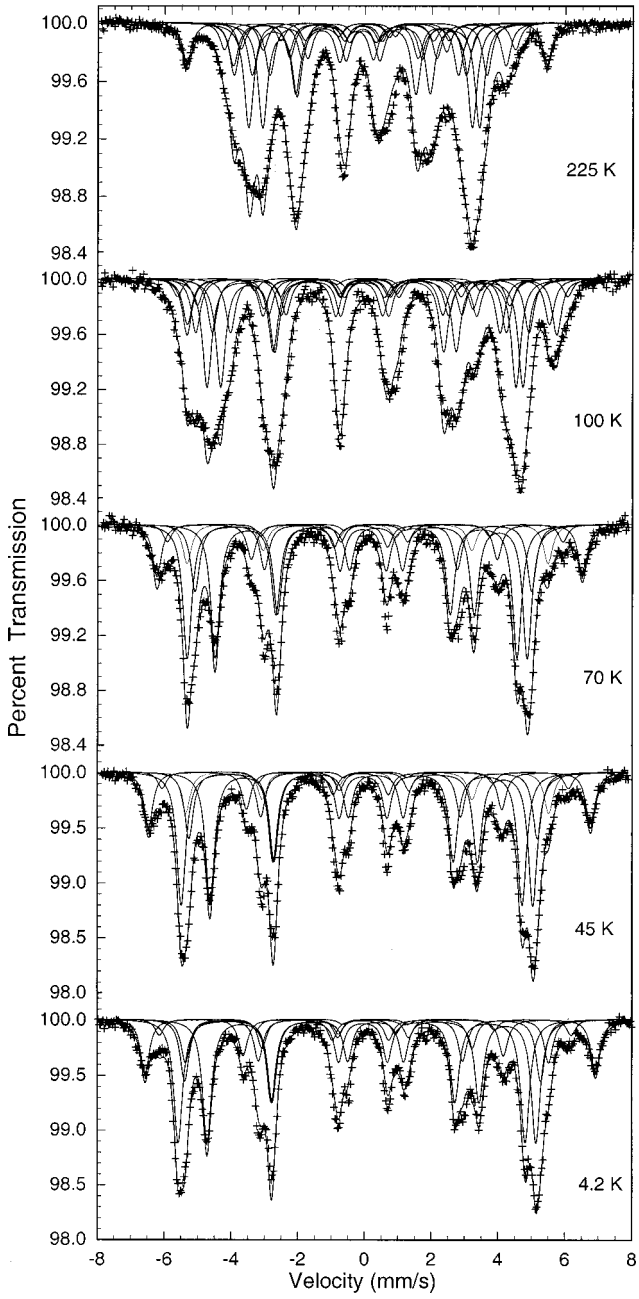

FIG. 4. The Mössbauer spectra of Tm_2Fe_{17} obtained at the indicated temperatures.

from five, at the lowest temperatures, to eight at the highest temperatures. Below 85 K, the iron magnetic moments in Tm_2Fe_{17} are parallel to the c axis of the unit cell, and hence the Mössbauer spectra are analyzed[10] with five sextets assigned to the crystallographically inequivalent $4e$, $4f$, $6g$, $12j$, and $12k$ iron sites and one additional sextet assigned to the α-iron impurity, with a relative area of $\sim$10%. In these fits, one single linewidth of 0.32 mm/s has been used, and the relative areas of the $6g$, $12j$, and $12k$ sextets have been constrained in the ratio 6:12:12. The isomer shifts, the hyperfine fields, the quadrupole interactions $e^2Qq/2$, and the angles θ between the principal axis of the electric field gradient tensor and the hyperfine field have been adjusted. The asymmetry parameter for the $4e$, $4f$, and $6g$ sites has been set equal to 0, whereas the asymmetry parameter for the $12j$ and $12k$ sites was set equal to 1 in agreement with the results[9] of the point charge calculation of the electric-field gradients in Ce_2Fe_{17}. The $e^2Qq/2$, θ, and η values were adjusted in agreement with the known values of the quadrupole splittings for the $4e$, $4f$, $6g$, $12j$, and $12k$ sites at 320 K. The fitted hyperfine parameters and relative areas are given in Table II. It should be noted that the θ angles for the $4e$ and $4f$ sites are 0, in agreement with the orientation of both the principal axis of the electric-field gradient tensor and the hyperfine field parallel to the c axis of the unit cell. The θ angles for the $6g$, $12j$, and $12k$ sites will be discussed below. Various preliminary fits indicated that the sign of $e^2Qq/2$ for the $4e$, $4f$, $6g$, and $12k$ sites was undoubtedly negative, whereas fits of similar quality could be obtained with either a positive or a negative $e^2Qq/2$ for the $12j$ site. In agreement with the results[9] of the point-charge calculation of the electric-field gradient in Ce_2Fe_{17} and with the analysis[10] of the 4.2 K spectrum of $Pr_2Fe_{17}H_3$, a spectrum which is very similar to the 4.2 K spectrum shown in Fig. 4, a positive sign is used.

Above 95 K, the iron magnetic moments are oriented within the basal plane of the unit cell, and hence the Mössbauer spectra have been analyzed[14,15] with nine sextets, eight assigned to the magnetically inequivalent $4e$, $4f$, $6g_4$, $6g_2$, $12j_8$, $12j_4$, $12k_8$, and $12k_4$ iron sites, and one assigned to the α-iron impurity, an impurity which has a relative area of $\sim$10%. Between 95 and 225 K, a single linewidth of 0.33 mm/s has been used, and the relative areas of the $6g_4$, $6g_2$, $12j_8$, $12j_4$, $12k_8$, and $12k_4$ sextets have been constrained in a ratio 4:2:8:4:8:4. The isomer shifts of the crystallographically equivalent but magnetically inequivalent sites have been constrained to be equal. The isomer shifts δ, the hyperfine fields, H, the quadrupole interactions $e^2Qq/2$, and the angles θ between the principal axis of the electric-field gradient tensor and the hyperfine field have been adjusted. The asymmetry parameter for the $4e$, $4f$, and $6g$ sites has been set equal to 0, whereas the asymmetry parameter for the $12j$ and $12k$ sites has been adjusted in agreement with the results[9] of the point charge calculation of the electric-field gradients in Ce_2Fe_{17}. The $e^2Qq/2$, θ, and η values have been adjusted in agreement with the known values of the quadrupole splittings for the $4e$, $4f$, $6g$, $12j$, and $12k$ sites at 320 K. The resulting hyperfine parameters and relative areas are given in Table II. It should be noted that the θ angles for the $4e$ and $4f$ sites are 90°, as expected if the iron magnetic moments and hyperfine fields are in the basal plane of the unit cell. The θ angles for the $6g_4$, $6g_2$, $12j_8$, $12j_4$, $12k_8$, and $12k_4$ sites will be discussed below.

At 85, 90, and 95 K, the spectra are mixture of axial and basal orientations of the iron magnetic moments. In a first approximation, the spectra obtained at 85 and 90 K have been analyzed as axial spectra, whereas the 95-K spectrum has been analyzed as a basal spectrum. A close visual inspection of the spectra indicates that the spin reorientation begins at $\sim$75 K and is complete at $\sim$100 K.

On the basis of the disorder observed[17] in Ho_2Fe_{17}, the expected relative areas of the $4e$, $4f$, $6g$, $12j$, and $12k$

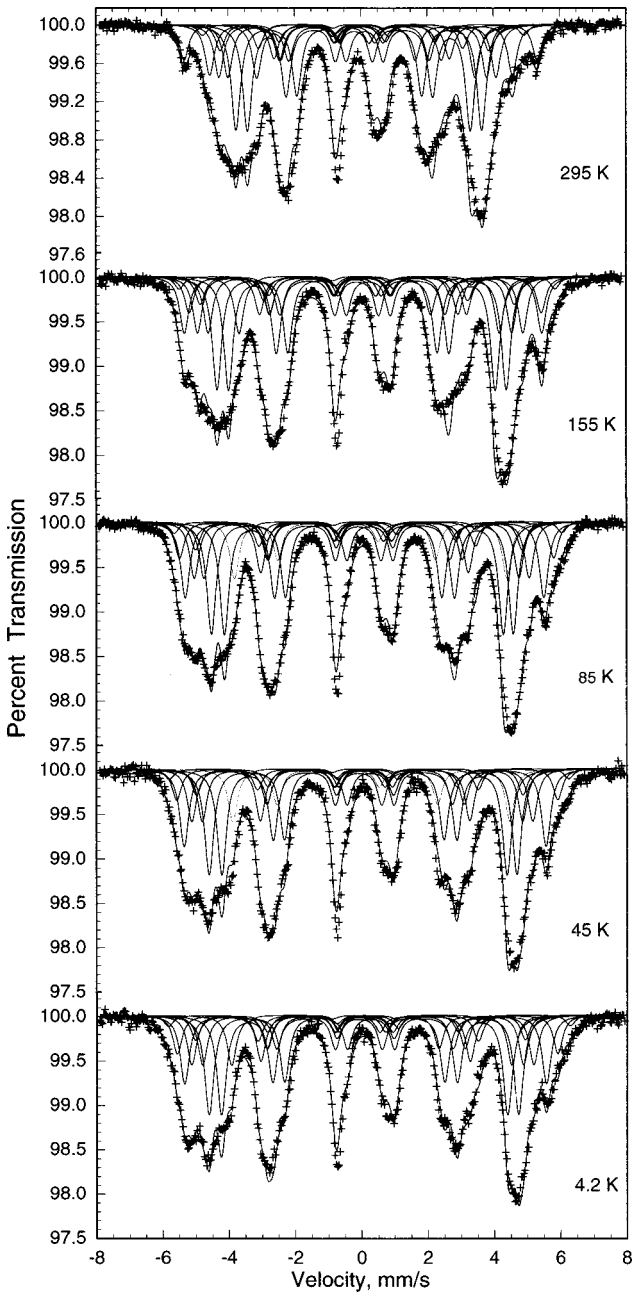

FIG. 5. The Mössbauer spectra of $Tm_2Fe_{17}D_{3.2}$ obtained at the indicated temperatures.

spectral components are 2.84, 9.79, 17.47, 34.95, and 34.95%, respectively. Even though the relative areas given in Table II have been adjusted, they do not deviate substantially from the expected areas. The observed $4e$ relative area, which is larger than the expected one, may indicate a more extensive disorder in Tm_2Fe_{17} than in Ho_2Fe_{17}, or a phase slightly richer in iron, in agreement with a broadening[17] of the homogeneity range of the R_2Fe_{17} phases with the increasing atomic number of the rare earth.

$Tm_2Fe_{17}D_{3.2}$. The Mössbauer spectra of $Tm_2Fe_{17}D_{3.2}$ obtained at 4.2, 45, 85, 155, and 295 K, are shown in Fig. 5. A visual comparison of Figs. 4 and 5 immediately indicates that the deuterium atoms have entered the structure, and that they have dramatic effects on the hyperfine parameters. In contrast, with the break in the temperature dependence of the Tm_2Fe_{17} spectra, the spectra of $Tm_2Fe_{17}D_{3.2}$ shown in Fig. 5 are broad, and show a smooth temperature dependence. At 4.2 K, the sharpness of the Mössbauer spectrum of Tm_2Fe_{17} has disappeared in $Tm_2Fe_{17}D_{3.2}$ because of the basal orientation of the iron magnetic moments, whereas at 295 K $Tm_2Fe_{17}D_{3.2}$ shows a magnetic spectrum because of its increased ordering temperature upon deuterium insertion. These Mössbauer spectra were analyzed[14,15] with eight sextets assigned to the magnetically inequivalent $4e$, $4f$, $6g_4$, $6g_2$, $12j_8$, $12j_4$, $12k_8$, and $12k_4$ iron sites, and one additional sextet assigned to the α-iron impurity, with a relative area of ~13%. One single linewidth of 0.33 mm/s has been fit, and the relative areas of the $6g_4$, $6g_2$, $12j_8$, $12j_4$, $12k_8$, and $12k_4$ sextets have been constrained in a ratio 4:2:8:4:8:4. The usual constraints on the isomer shifts and relative areas of crystallographically equivalent and magnetically inequivalent sites have been applied. Because the quadrupole interactions in $Tm_2Fe_{17}D_{3.2}$ are not known, as was the case for Tm_2Fe_{17}, quadrupole shift values with θ equal to zero have been fit, except for the $4e$ and $4f$ sites, for which quadrupole interaction values with η equal to zero and θ equal to 90° have been fit. The resulting hyperfine parameters and relative areas are given in Table III. The fitted relative areas given in Table III agree very well with the expected relative areas given above on the basis of the disorder observed[16] in Ho_2Fe_{17}.

V. DISCUSSION AND CONCLUSION

Both the ac susceptibility and the Mössbauer spectral measurements confirm the presence of a spin reorientation in Tm_2Fe_{17} below 100 K. From the temperature dependence of the Mössbauer spectra, a spin-reorientation temperature of 90 K is estimated. Above 95 K, the magnetic moments are oriented within the basal plane; below 80 K they are parallel to the c axis, as a result of the dominant thulium sublattice anisotropy. The spin-reorientation temperature of 90 K is larger than the earlier reported[2,5,25] value of 72 K. This difference may result from the choice[2,5,25] of the inflection point in the temperature dependence of the ac susceptibility as the spin-reorientation temperature, and from a difference in sample stoichiometry, a difference which is in agreement with the broad homogeneity range[26] of Tm_2Fe_{17}.

Both the ac susceptibility and the Mössbauer spectral measurements on $Tm_2Fe_{17}D_{3.2}$ reveal that the easy magnetization axis does not change between 4.2 and 295 K, and is oriented within the basal plane. Hence, in contrast to the insertion of carbon or nitrogen, both of which increase the spin-reorientation temperature, the insertion of deuterium suppresses the spin reorientation. Hence carbon and nitrogen have opposite effects on the thulium anisotropy as compared with deuterium. Although all three interstitial elements expand the lattice, their different chemical natures have different influences on the crystal electric-field gradient at the rare-earth site in R_2Fe_{17}. In the case of gadolinium, it was shown that carbon and nitrogen,[27–29] have an opposite effect on the crystal electric field gradient to that of hydrogen.[30] In the

TABLE III. Mössbauer spectral hyperfine parameters for $Tm_2Fe_{17}D_{3.2}$.

	T, K	$4f$	$4e$	$6g_4$	$6g_2$	$12j_8$	$12j_4$	$12k_8$	$12k_4$	Wt. Ave.
H, kOe	4.2	355.6	375.0	299.7	308.0	277.5	319.5	278.8	261.7	297.4
	45	356.0	373.0	299.3	305.0	275.6	318.5	278.3	258.9	296.1
	85	349.6	362.0	294.3	305.0	269.8	312.9	272.7	254.4	290.7
	120	341.2	356.0	289.3	299.0	265.4	308.7	266.8	248.8	285.3
	155	329.0	351.0	283.6	293.5	259.5	304.0	260.0	243.0	278.8
	225	307.0	332.0	267.3	274.0	242.8	285.9	244.8	226.0	261.5
	295	283.0	300.0	241.9	251.0	219.0	259.0	219.0	203.9	236.4
δ,[a] mm/s	4.2	0.180	0.150	−0.005	−0.005	0.075	0.075	0.085	0.085	0.076
	45	0.180	0.150	−0.020	−0.020	0.071	0.071	0.083	0.083	0.071
	85	0.174	0.142	−0.035	−0.035	0.069	0.069	0.073	0.073	0.063
	120	0.160	0.128	−0.050	−0.050	0.057	0.057	0.061	0.061	0.050
	155	0.145	0.120	−0.065	−0.065	0.040	0.040	0.045	0.045	0.034
	225	0.095	0.070	−0.105	−0.105	0.000	0.000	0.002	0.002	−0.008
	295	0.025	0.005	−0.145	−0.145	−0.040	−0.040	−0.050	−0.050	−0.055
QS,[b] mm/s	4.2	0.04	−0.30	0.08	−0.08	0.34	−0.10	−0.38	0.42	-
	45	0.04	−0.30	0.08	−0.08	0.34	−0.10	−0.38	0.42	-
	85	0.04	−0.30	0.08	−0.08	0.32	−0.11	−0.38	0.42	-
	120	0.04	−0.30	0.08	−0.08	0.32	−0.11	−0.37	0.42	-
	155	0.04	−0.30	0.08	−0.08	0.32	−0.11	−0.37	0.42	-
	225	0.04	−0.30	0.09	−0.08	0.32	−0.11	−0.37	0.42	-
	295	0.04	−0.30	0.09	−0.08	0.32	−0.11	−0.35	0.42	-
Area, %	4.2	9.1	2.5	11.8	5.8	23.6	11.8	23.6	11.8	-
	45	7.6	2.4	12.0	6.0	24.0	12.0	24.0	12.0	-
	85	7.6	2.4	12.0	6.0	24.0	12.0	24.0	12.0	-
	120	7.8	2.4	12.0	6.0	24.0	12.0	24.0	12.0	-
	155	7.7	2.7	12.0	6.0	24.0	12.0	24.0	12.0	-
	225	8.8	2.7	11.8	5.8	23.6	11.8	23.6	11.8	-
	295	11.2	2.6	11.5	5.7	23.0	11.5	23.0	11.5	-

[a]The isomer shifts are given relative to room-temperature α-iron foil.
[b]Quadrupole shifts values, except for the $4e$ and $4f$ sites for which QS is the quadrupole splitting, ΔE_Q, with $\theta = 90°$.

case of erbium and thulium, ^{166}Er and ^{169}Tm Mössbauer spectral measurements[3,31] have shown that the second-order crystal-field parameter A_2^0 becomes more negative upon carbon or nitrogen insertion into Er_2Fe_{17} and Tm_2Fe_{17}. Hence, because deuterium insertion suppresses the spin reorientation in Tm_2Fe_{17}, we can conclude that A_2^0 either becomes more positive or is essentially zero, as was observed[30] in $Gd_2Fe_{17}H_x$, with increasing x.

The fits shown in Figs 3, 4, and 5, with either five or eight spectral components, are certainly not unique, but they are based on reasonable assumptions and constraints on the hyperfine parameters. We assumed both that the relative areas of the $6g$, $12j$, and $12k$ iron sites are proportional to their crystallographic degeneracies and that the quadrupole splittings, ΔE_Q, do not change at either the ordering temperature or the spin-reorientation temperature of Tm_2Fe_{17}. We constrain the isomer shifts of magnetically inequivalent and crystallographically equivalent iron sites to be equal. As shown below, these assumptions and constraints lead to an assignment of the different spectral components to the different iron sites, an assignment which is supported by the temperature dependence of the hyperfine parameters and the changes in the observed spectra with changes in the rare-earth atom in R_2Fe_{17}.

The temperature dependence of the isomer shift of the five different iron sites in Tm_2Fe_{17} is shown in Fig. 6. At all temperatures, the sequence of the isomer shifts, $4f > 12k$

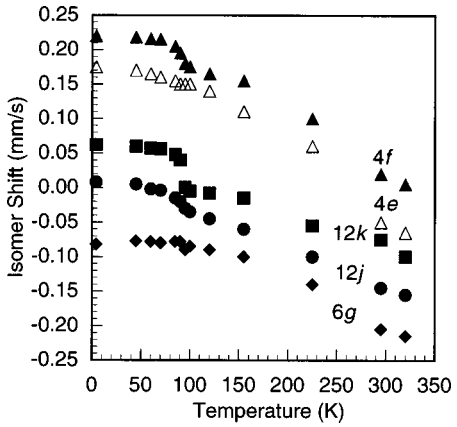

FIG. 6. The temperature dependence of the isomer shifts in Tm_2Fe_{17}.

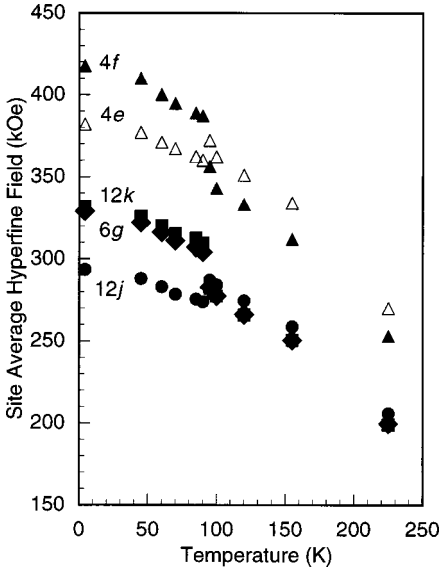

FIG. 7. The temperature dependence of the site average hyperfine fields in Tm_2Fe_{17}.

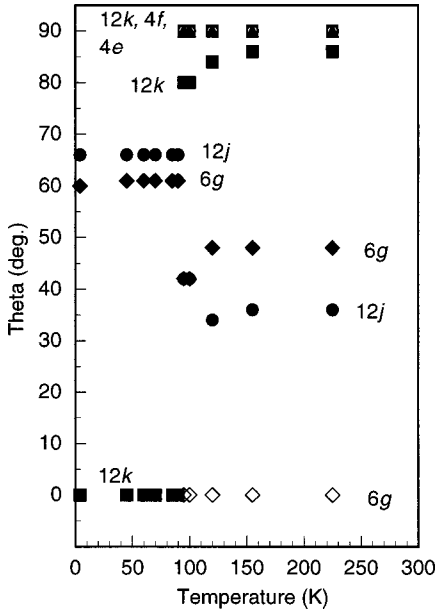

FIG. 8. The temperature dependence of the θ angles in Tm_2Fe_{17}.

$>12j>6g$, agrees with the sequence observed[9,10,32,33] in the other R_2Fe_{17} and with the sequence of Wigner-Seitz cell volumes. The $4e$ isomer shift is smaller than the $4f$ isomer shift, as was observed[14] in Dy_2Fe_{17} but not[15] in Er_2Fe_{17}. The temperature dependence of the five isomer shifts follows a typical second-order Doppler shift behavior with only a discontinuity near the spin-reorientation temperature. This discontinuity, which is artificially enhanced by the rather poor fits obtained at 85, 90, and 95 K, may be related to a small anisotropic magnetostriction of the unit cell at the spin-reorientation temperature, which manifests itself by the negative thermal expansion coefficient observed[34] between 231 and 4.2 K.

The temperature dependence of the site average hyperfine fields in Tm_2Fe_{17} is shown in Fig. 7. The $4e$ and $4f$ hyperfine fields are the largest observed[9–11,14,15,32,33] in the other R_2Fe_{17} compounds. The effect of the spin reorientation on the hyperfine fields is very clear at 92 K. Above 92 K, the hyperfine field sequence, $4f>12j>6g\approx12k$, follows the sequence observed[9–11,14,15,32,33] in the other R_2Fe_{17} compounds, and is in agreement with the sequence of iron near neighbors, $12>10=10>9$. Below 92 K, rather surprisingly the $12j$ hyperfine field is the smallest. The assignment of the $12j$ and $12k$ sites has been made on the basis of the isomer shift and the sign of the quadrupole interaction, and hence a reversed assignment of the fields is difficult without compromising other highly viable portions of the analysis.

As observed[10,11,33] earlier in $Pr_2Fe_{17}H_x$, with x between 3 and 5, and in $Sm_2Fe_{17}N_3$, all of which exhibit axial orientations of the iron magnetic moments and hyperfine fields, the hyperfine field at the dumbbell iron sites, $4f$ or $6c$, is significantly larger than in the R_2Fe_{17} compounds, which exhibit a basal orientation of the iron magnetic moments. In addition, all the hyperfine fields show a significant break in their temperature dependence near the spin-reorientation temperature. The $4f$, $6g$, and $12k$ hyperfine fields decrease when increasing the temperature through the spin reorientation, whereas the $4e$ and $12j$ hyperfine fields increase; a similar behavior was observed[11] in $Pr_2Fe_{17}H_3$. The $4f$ iron atoms have both orbital and spin contributions[35] to their magnetic moments and their respective contributions to the hyperfine field are of opposite sign. Below the spin reorientation, the orbital contribution is reduced as a consequence of the rotation of the iron moment away from their easy direction within the basal plane toward their hard direction parallel to the c axis. An additional contribution to the hyperfine field is the transferred field induced by the thulium magnetic moment, which increases rapidly with decreasing temperature, as indicated by neutron-diffraction measurements[34] and our magnetization measurements at 30 kOe, see the inset of Fig. 1. The combination of the transferred and orbital contributions, which both are temperature dependent, leads to a substantial increase of the hyperfine field of ~45 kOe, an increase which is in perfect agreement[2] with the earlier reported value of 44 kOe.

The quadrupole interactions, given by the expression,

$$\frac{e^2Qq}{2}\left(1+\frac{\eta^2}{3}\right)^{1/2},$$

have been kept essentially constant between 4.2 and 320 K and they agree with those measured[9,15,36] in Ce_2Fe_{17}, Pr_2Fe_{17}, and in Er_2Fe_{17}.

The temperature dependence of the θ angle, i.e., the angle between the principal axis of the electric field gradient tensor and the hyperfine field, assumed to be parallel to the iron magnetic moment at the different iron sites in Tm_2Fe_{17}, is shown in Fig. 8. As already noted above, the θ angles for the $4e$ and $4f$ sites of zero and 90° below and above the spin-reorientation temperature, respectively, are in agreement with a principal axis of the electric-field gradient V_{zz}, which is parallel to the c axis of the unit cell and a hyperfine field, which is parallel and perpendicular to the c axis of the unit

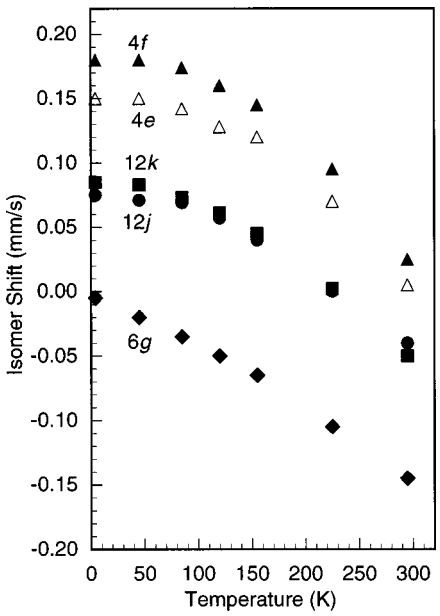

FIG. 9. The temperature dependence of the isomer shifts in $Tm_2Fe_{17}D_{3.2}$.

cell below and above the spin-reorientation temperature, respectively. Below 90 K, the principal axis of the electric-field gradient, V_{zz}, at the $6g$, $12j$, and $12k$ sites, makes angles of 61°, 66°, and 0°, respectively, with the hyperfine field which is assumed to be parallel to the c axis of the unit cell. These values are different from those calculated[9] for rhombohedral Ce_2Fe_{17}. The random substitution of rare-earth atoms by $4e$ iron pairs in hexagonal Tm_2Fe_{17} modifies the electric charge distribution around the iron atoms and hence the direction of V_{zz} relative to the c axis.

Above 92 K, the $6g$, $12j$, and $12k$ sites are subdivided into two magnetically inequivalent sites with different θ angles. Two preferential directions of the hyperfine field within the basal plane, along [100] and [−110], were observed[5,32,34] in the Mössbauer spectra of Nd_2Fe_{17} and Pr_2Fe_{17}, respectively. The Mössbauer spectra of Tm_2Fe_{17} above 92 K are similar to those of Nd_2Fe_{17} and hence, the iron magnetic moments are mainly along [100]. A comparison of the Mössbauer spectra of $Tm_2Fe_{17}D_{3.2}$ with those[10,12] of $Nd_2Fe_{17}H_3$ and $Pr_2Fe_{17}H_x$ indicates that the iron magnetic moments are also along [100] in $Tm_2Fe_{17}D_{3.2}$.

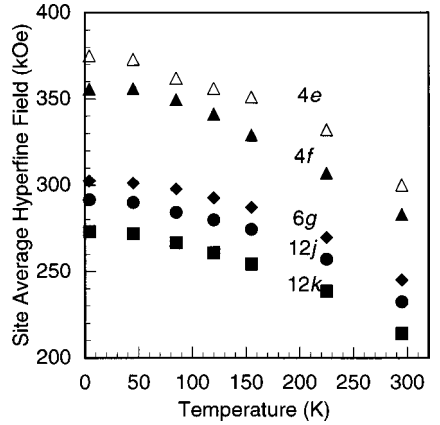

FIG. 10. The temperature dependence of the site average hyperfine fields in $Tm_2Fe_{17}D_{3.2}$.

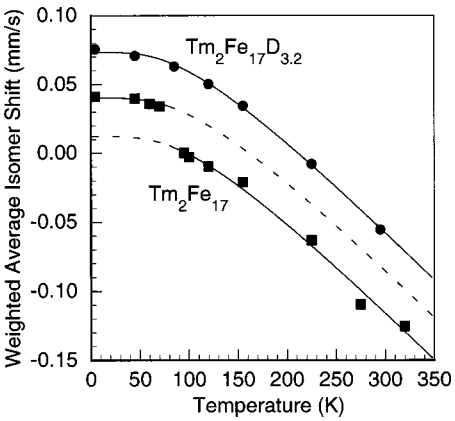

FIG. 11. The temperature dependence of the weighted average isomer shifts in Tm_2Fe_{17} and $Tm_2Fe_{17}D_{3.2}$. The solid and dotted lines are second-order Doppler shift fits as described in the text.

The smooth temperature dependence of the isomer shifts in $Tm_2Fe_{17}D_{3.2}$ is shown in Fig. 9. The sequence of isomer shifts, $4f>4e>12k\approx12j>6g$, is similar to the sequence observed[14] in $Dy_2Fe_{17}H_{3.8}$, with the exception of the $4e$ site. This site has a very small relative area in the Mössbauer spectra and hence the error in its isomer shift may be larger than for the other sites.

The temperature dependence of the site average hyperfine fields in $Tm_2Fe_{17}D_{3.2}$ is shown in Fig. 10. The sequence of hyperfine fields, $4e>4f>6g>12j>12k$, is identical to the sequence observed[14] in $Dy_2Fe_{17}H_{3.8}$.

The effect of deuterium insertion in Tm_2Fe_{17} on the weighted average isomer shift is illustrated in Fig. 11. Specifically, the weighted average isomer shift increases upon deuterium insertion because of the lattice expansion, and the resulting decrease in the s-electron density at the iron nuclei. The solid lines in Fig. 11 were calculated[37] for a second-order Doppler shift model. The smooth temperature dependence of the weighted average isomer shift in $Tm_2Fe_{17}D_{3.2}$ is

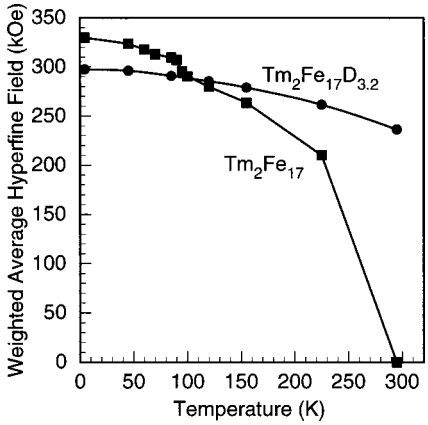

FIG. 12. The temperature dependence of the weighted average hyperfine fields in Tm_2Fe_{17} and $Tm_2Fe_{17}D_{3.2}$. The solid lines are guides to the eyes.

well fit with an iron effective vibrating mass of 57 g/mol and a Mössbauer lattice temperature of 386 K. Because of the break in the temperature dependence of the weighted average isomer shift in Tm_2Fe_{17} at 90 K, the fit was carried out in two temperature ranges, as shown by the two curves in Fig. 11. Preliminary fits showed that the iron effective vibrating masses were close to 57 g/mol, and they were subsequently constrained to this value. The corresponding Mössbauer lattice temperatures are ~410 K in both the low- and high-temperature regions.

The effect of deuterium insertion in Tm_2Fe_{17} on the weighted average hyperfine field is illustrated in Fig. 12. Below 92 K, the weighted average hyperfine field in Tm_2Fe_{17} is larger than in $Tm_2Fe_{17}D_{3.2}$. This small decrease in the saturation hyperfine field upon deuterium insertion indicates that there is no increase in the iron magnetic moments, as suggested by the saturation magnetization measured in both compounds; see Sec. III. Because the ordering temperature of Tm_2Fe_{17} is 280 K, its weighted average hyperfine field decreases rapidly to zero, whereas the weighted average hyperfine field in $Tm_2Fe_{17}D_{3.2}$ decreases only slightly between 4.2 and 295 K.

ACKNOWLEDGMENTS

The authors thank Dr. D. Hautot and Z. Lin for help in obtaining the Mössbauer spectra. G.J.L. thanks the U.S. National Science Foundation for Grant Nos. DMR95-21739 and INT-9815138, and the 'Fonds National de la Recherche Scientifique,' Brussels, Belgium, for support during a sabbatical leave in 2000-2001. O.I. thanks the 'Centre National de la Recherche Scientifique, France' for grant action initiative No. 7418.

*Email address: fgrandjean@ulg.ac.be
†Email address: isnard@labs.polycnrs-ge.fr
‡Email address: glong@umr.edu

[1] P. C. M. Gubbens, A. M. van der Kraan, J. J. van Loef, and K. H. J. Buschow, J. Magn. Magn. Mater. **67**, 255 (1987).
[2] P. C. M. Gubbens and K. H. J. Buschow, Phys. Status Solidi A **34**, 729 (1976).
[3] P. C. M. Gubbens, A. M. van der Kraan, T. H. Jacobs, and K. H. J. Buschow, J. Magn. Magn. Mater. **80**, 265 (1989).
[4] D. Givord and R. Lemaire, C. R. Acad. Sci. (Paris) **274**, 1166 (1972).
[5] P. C. M. Gubbens, Ph.D. thesis, Delft University Press, 1977.
[6] O. Isnard, S. Miraglia, and D. Fruchart, J. Magn. Magn. Mater. **140–144**, 981 (1995).
[7] P. C. M. Gubbens, A. A. Moolenaar, T. H. Jacobs, and K. H. J. Buschow, J. Alloys Compd. **176**, 115 (1991).
[8] B. P. Hu, H. S. Li, H. Sun, J. F. Lawler, and J. M. D. Coey, Solid State Commun. **76**, 587 (1990).
[9] D. Hautot, G. J. Long, F. Grandjean, and O. Isnard, Phys. Rev. B **62**, 11 731 (2000).
[10] D. Hautot, G. J. Long, F. Grandjean, O. Isnard, and S. Miraglia, J. Appl. Phys. **86**, 2200 (1999).
[11] F. Grandjean, D. Hautot, G. J. Long, O. Isnard, S. Miraglia, and D. Fruchart, J. Appl. Phys. **85**, 4654 (1999).
[12] F. Grandjean, G. J. Long, S. Mishra, O. A. Pringle, O. Isnard, S. Miraglia, and D. Fruchart, Hyperfine Interact. **95**, 571 (1995).
[13] D. Hautot, G. J. Long, F. Grandjean, O. Isnard, and D. Fruchart, J. Magn. Magn. Mater. **202**, 107 (1999).
[14] O. Isnard, D. Hautot, G. J. Long, and F. Grandjean, J. Appl. Phys. **88**, 2750 (2000).
[15] F. Grandjean, O. Isnard, D. Hautot, and G. J. Long, Phys. Rev. B **63**, 014406 (2001).
[16] O. Isnard, S. Miraglia, J. L. Soubeyroux, D. Fruchart, and A. Stergiou, J. Less-Common Met. **162**, 273 (1990).
[17] O. Isnard, S. Miraglia, J. L. Soubeyroux, and D. Fruchart, Solid State Commun. **87**, 13 (1992).
[18] O. Isnard, S. Miraglia, J. L. Soubeyroux, D. Fruchart, and P. L'Héritier, J. Magn. Magn. Mater. **137**, 151 (1994).
[19] C. Rillo, F. Lera, A. Badia, L. Angurel, J. Bartolomé, F. Palacio, R. Navarro, and A. J. Duyneveldt, in *Susceptibility of Superconductors and Other Spin Systems*, edited by R. A. Hein, J. L. Francavilla, and D. H. Liebenberg (Plenum, New York, 1992).
[20] A. Barlet, J. C. Genna, and P. Lethuillier, Cryogenics **31**, 801 (1991).
[21] D. Givord and R. Lemaire, IEEE Trans. Magn. **10**, 109 (1974).
[22] D. Givord, Ph.D. thesis, University of Grenoble, 1973.
[23] D. Givord, R. Lemaire, J. M. Moreau, and E. Rouault, J. Less-Common Met. **29**, 361 (1972).
[24] F. J. Lazaro, L. M. Garcia, F. Luis, J. Bartolomé, D. Fruchart, O. Isnard, S. Miraglia, S. Obbade, and K. H. J. Buschow, J. Magn. Magn. Mater. **101**, 372 (1991).
[25] R. Grössinger, X. C. Kou, T. H. Jacobs, and K. H. J. Buschow, J. Appl. Phys. **69**, 5596 (1991).
[26] K. H. J. Buschow, J. Less-Common Met. **11**, 204 (1966).
[27] M. W. Dirken, R. C. Thiel, L. J. D. de Jongh, T. H. Jacobs, and K. H. J. Buschow, J. Magn. Magn. Mater. **155**, 339 (1989).
[28] M. W. Dirken, R. C. Thiel, R. Coehoorn, T. H. Jacobs, and K. H. J. Buschow, J. Magn. Magn. Mater. **94**, L15 (1992).
[29] F. M. Mulder, R. C. Thiel, R. Coehoorn, T. H. Jacobs, and K. H. J. Buschow, J. Magn. Magn. Mater. **117**, 413 (1992).
[30] O. Isnard, P. Vuillet, A. Blaise, J. P. Sanchez, S. Miraglia, and D. Fruchart, J. Magn. Magn. Mater. **131**, 83 (1994).
[31] P. C. M. Gubbens, A. A. Moolenaar, G. J. Boender, A. M. van der Kraan, T. H. Jacobs, and K. H. J. Buschow, J. Magn. Magn. Mater. **97**, 69 (1991).
[32] G. J. Long, O. A. Pringle, F. Grandjean, and K. H. J. Buschow, J. Appl. Phys. **72**, 4845 (1992).
[33] G. J. Long, S. Mishra, O. A. Pringle, F. Grandjean, and K. H. J. Buschow, J. Appl. Phys. **75**, 5994 (1994).
[34] J. B. A. A. Elemans and K. H. J. Buschow, Phys. Status Solidi A **24**, K125 (1974).
[35] J. Deportes, B. Kebe, and R. Lemaire, J. Magn. Magn. Mater. **54–57**, 1089 (1986).
[36] G. J. Long, O. A. Pringle, F. Grandjean, W. B. Yelon, and K. H. J. Buschow, J. Appl. Phys. **74**, 504 (1993).
[37] G. J. Long, D. Hautot, F. Grandjean, D. T. Morelli, and G. P. Meisner, Phys. Rev. B **60**, 7410 (1999).